

Journal of Biomedical Optics

SPIDigitalLibrary.org/jbo

***In vivo* therapy monitoring of experimental rheumatoid arthritis in rats using near-infrared fluorescence imaging**

Sonja Vollmer
Ines Gemeinhardt
Axel Vater
Beatrix Schnorr
Jörg Schnorr
Jan Voigt
Bernd Ebert

In vivo therapy monitoring of experimental rheumatoid arthritis in rats using near-infrared fluorescence imaging

Sonja Vollmer,^{a,*} Ines Gemeinhardt,^b Axel Vater,^{a,c} Beatrix Schnorr,^b Jörg Schnorr,^b Jan Voigt,^{d,e} and Bernd Ebert^d

^aBayer Pharma AG, Global Drug Discovery, Berlin 13353, Germany

^bCharité–Universitätsmedizin Berlin, Department of Radiology 10117, Germany

^cNOXXON Pharma AG, Drug Discovery, Berlin 10589, Germany

^dPhysikalisch-Technische Bundesanstalt, Department of Biomedical Optics, Berlin 10587, Germany

^eMedical School Hannover, Department of Radiotherapy and Special Oncology, Hannover 30625, Germany

Abstract. An *in vivo* near-infrared fluorescence (NIRF) imaging technique is described for therapy monitoring of ankle joints affected by collagen-induced arthritis, a model of human rheumatoid arthritis. Arthritis was induced in rats by intradermal injections of collagen and Freund's incomplete adjuvant. For *in vivo* imaging, the nonspecific NIR dye tetrasulfocyanine (TSC) was used. Prior to and after treatment with a nonsteroidal anti-inflammatory drug, *meloxicam*, or analgesic drug, *tramadol hydrochloride* (which served as no-therapy control), normalized fluorescence intensities of each ankle joint were measured. Additionally, each ankle joint was characterized by clinical arthritis scoring and histopathology. Over a 3-week treatment period, a significant difference in disease progression between animals treated with *meloxicam* and *tramadol hydrochloride* was detected. A statistically significant improvement in ankle joint pathology from high- or moderate-grade to moderate- or low-grade upon *meloxicam* therapy, as determined by clinical evaluation, translated into a significant decrease in fluorescence intensity. In contrast, all arthritic joints of the no-therapy control group deteriorated to high-grade arthritis with high-fluorescence intensities in NIRF imaging. © The Authors. Published by SPIE under a Creative Commons Attribution 3.0 Unported License. Distribution or reproduction of this work in whole or in part requires full attribution of the original publication, including its DOI. [DOI: 10.1117/1.JBO.19.3.036011]

Keywords: near-infrared fluorescence imaging; rheumatoid arthritis; anti-inflammatory treatment; therapy response monitoring.

Paper 130847R received Nov. 27, 2013; revised manuscript received Jan. 27, 2014; accepted for publication Feb. 11, 2014; published online Mar. 17, 2014.

1 Introduction

Rheumatic diseases have a prevalence of about 1% in the Western world.¹ The prevalence increases with age, reaching about 2% in men and women over 55 years. Women are affected two to three times more frequently than men. There is no cure for rheumatoid arthritis (RA), and the etiology of inflammatory rheumatic joint diseases is still elusive. Pathogen-related, genetic, and autoimmune hypotheses are being discussed. Apart from the enormous spread of this endemic disease, high costs for treatment and rehabilitation have to be considered,² e.g., 50% of the patients are disabled after 20 years.³ Although RA is serious, potentially crippling and commonly disabling, comprehensive diagnosis and optimized therapies are hindered by lack of cost-efficient and powerful joint imaging technologies that allow quantitative monitoring of therapeutic effects on inflammation.⁴

Histopathological studies of rheumatic joints generally show chronic proliferative synovitis with fibrin deposition in and around the synovial membrane and the articular cartilage as the hallmark symptom of RA. Synovitis is characterized by persistent vasodilatation and increased capillary permeability.⁵ As the disease progresses, the synovial lining develops into a

hypertrophic, edematous, and highly vascularized tissue layer, known as pannus, which invades and degrades adjacent cartilage and bone.⁶

The diagnosis of inflammatory joint disease is currently based on the patient's history, clinical findings, laboratory results, and conventional radiography. X-ray examination has for decades been the gold standard for detection and assessment of joint damage and continues to be the primary imaging technique for the diagnosis and evaluation of arthritis. This modality, however, can only demonstrate the time-integrated record of joint damage that tends to develop late in the course of the disease.⁴ Therefore, X-ray is of limited value for early diagnosis or therapy monitoring, for which there is an increasing demand in patients treated with today's potent biologics. Even though the majority of patients benefit from biologic therapy, up to one-third has only minor, transient clinical improvement, or experiences no benefit at all.^{7–9} Moreover, adverse effects and costs may be high, making a reliable, radiation-free, and fast imaging modality for therapy monitoring highly welcome. The information provided by such a modality could help in stratifying treatment and tailoring it to the individual patient.¹⁰

In the last years, optical imaging methods based on near-infrared fluorescence (NIRF) have emerged as promising new noninvasive arthritis imaging modalities,^{11,12} supplementing the time-consuming, expensive, and/or radiation-using modalities such as magnetic resonance imaging (MRI), positron

*Address all correspondence to: Sonja Vollmer, E-mail: sonja.vollmer@bayer.com

emission tomography (PET), and ultrasound (US). Only recently, Xiralite® (mivenion GmbH, Berlin, Germany), a commercial NIRF system, has demonstrated its potential in imaging by microcirculation assessment in RA patients in several clinical studies in comparison with clinical examination, US, and contrast-enhanced MRI.¹³ Here, we report the results of the first NIRF imaging therapy monitoring study, in which we used tetrasulfocyanine (TSC) dye for monitoring meloxicam treatment in rats with collagen-induced arthritis (CIA).

2 Experimental

2.1 Animals

Animals used in this study were maintained in accordance with the guide for the care and use of laboratory animals published by the U.S. National Institutes of Health (NIH Publication NO. 85-23, revised 1996). All experiments were approved by the Local Animal Welfare Committee.

The arthritis studies were performed in female Lewis rats with a body weight of (175 ± 15) g (Charles River Laboratories, Sulzfeld, Germany) fed a normal diet.

2.2 Animal Model

RA was induced in 11 female Lewis rats by intradermal collagen injections. Three animals served as controls. CIA was induced as described elsewhere.¹⁴ Control injections were performed in the same way as the collagen injections.¹⁴ After 1 week, the procedure was repeated to boost the immune response. From previous experiments, it is known that arthritis develops 13 to 15 days after the first collagen injection, but is highly variable in severity. Animals may show different degrees of arthritis in the right- and left-ankle joint, or there may be animals without signs of clinical or histological changes in one or both joints.

Based on macroscopic and microscopic patterns, CIA progression was divided into three stages: (1) preclinical (from first collagen injection to clinically evident disease onset), (2) acute clinical [from disease onset (day 0) to day 14], and (3) chronic clinical (after day 14), where clinical (hind and fore paw swelling) and structural (inflammation and articular erosions in hind paws) evidence of joint involvement plateaus.¹⁵

Skeletal erosion begins 1 to 2 days after the onset of paw swelling and is associated with acute synovitis. Left untreated, cartilage matrix degeneration, and bone attrition progress rapidly. The widespread formation of osteophytes along the periosteal surface may eventually result in fusion (ankylosis) of the affected joints with joint deformities resulting in a significant reduction of mobility.¹⁶ Hence, the study duration was restricted to 3 weeks to include the acute and chronic phases of rat CIA. Symptomatic rats received analgesic treatment. As the study aimed at monitoring the response to treatment, only rats with significant arthritis symptoms were assigned to the “meloxicam” group, while presymptomatic or mildly to moderately affected animals were selected for the “no-therapy control” group, permitting monitoring of disease progression.

2.3 Arthritis Evaluation

Animals were observed daily for the onset of arthritis with respect to swelling, erythema, gait analysis, and functional impairment of the distal joints, in particular the tibiotarsal joints. A 4-point arthritis scale was used for grading the clinical symptoms of each hind paw as follows: “without arthritis signs” (no

clinical symptoms), “low-grade arthritis” (mild swelling, erythema, and functional deficits), “moderate arthritis” (moderate swelling, erythema, and functional deficits), or “high-grade arthritis” (severe swelling with erythema and reduced mobility).¹⁴

2.4 Treatment

Tramadol hydrochloride is a centrally acting synthetic opioid analgesic used to treat moderate to moderately severe pain with no anti-inflammatory effect. Tramadol hydrochloride (Tramal®, Grünenthal GmbH, Aachen, Germany) was administered to rats subcutaneously at a dose of 10 mg/kg body weight/day upon onset of clinical symptoms.

Meloxicam is a nonsteroidal anti-inflammatory drug with analgesic effects and is especially suitable for the treatment of arthritis in animals.¹⁷ Meloxicam (Metacam®, Boehringer Ingelheim Vetmedica GmbH, Ingelheim, Germany) was administered to rats subcutaneously at a dose of 0.5 mg/kg body weight/day after assignment to the meloxicam treatment group.

2.5 Histology

For histological workup, the hind legs of the animals were removed and fixed in 4% buffered formaldehyde solution (Mallinckrodt Baker, Deventer, The Netherlands).

Subsequently, the specimens were placed in ethylenediamine tetra-acetic acid decalcifying solution (Herbeta Arzneimittel, Berlin, Germany) for 5 weeks at 60°C. The solution was changed every week. The decalcified hind legs were embedded in paraffin; thereafter, about 4- μ m thick histological sections were cut and stained with hematoxylin and eosin.

The histopathological specimens were assessed for signs of arthritis using the following criteria: synovitis, peri-arthritis, tenosynovitis, periostitis, and cartilage/bone destruction. Each criterion was graded semiquantitatively by one reader blinded to NIRF values as well as clinical scores. Each joint was graded as follows: 0, no arthritis; 1 to 5, low-grade arthritis; 6 to 10, moderate arthritis; and 11 to 15, high-grade arthritis.^{14,18}

2.6 Fluorescent Dye

The nonspecific NIRF dye is a TSC dye based on an indotricarbocyanine (ITCC) chromophore. TSC is a low-molecular weight dye (836.9 g/mol) with both anionic and hydrophilic properties.^{19,20} In phosphate-buffered saline, TSC shows an absorption maximum at $\lambda_{\text{abs}} = 755$ nm and a fluorescence emission maximum at $\lambda_{\text{em}} = 778$ nm. The dye was dissolved in phosphate-buffered saline and was diluted with physiological saline solution. TSC was administered intravenously at a dose of 1 μ mol/kg body weight in a volume of 0.2 ml per 100 g body weight.

2.7 In Vivo NIRF Imaging

The NIRF laser imaging system was described previously.¹⁴ Rats were anesthetized prior to and during the imaging procedure as described before.¹⁴ Imaging was performed before and 30 min after TSC administration. A solid, polymeric cube containing the TSC-related NIR dye ITCC was placed next to each animal as reference. Acquired NIRF intensity data were digitally stored. Each animal was subjected to NIRF imaging prior to and after 2 and 3 weeks of therapy. Upon completion of the final imaging, the anesthetized rats were euthanized by an intracardiac injection of

0.5 ml of embutramide/mebezonium/tetracaine (T61® Intervet Deutschland GmbH, Unterschleissheim, Germany).

2.8 Data Analysis and Statistics

Four circular regions of interest (ROIs) with a constant diameter of 20 pixels were defined (see circles in Fig. 1): the left- and right-ankle joints with the center of the ROI positioned over the external malleolus, the tail base, and the reference cube on the left side.

Mean fluorescence intensities I_F were the average of all the fluorescence intensity values of pixels covered by the ROI of a particular region under investigation divided by the number of pixels. For quantitative analysis, the fluorescence intensities of the ankle joints were normalized to the background (I_{NF}), i.e., to the fluorescence intensity of the tail, to compensate for laser fluctuations and the decay of dye concentration. This ratio was calculated as

$$I_{NF} = I_F(\text{joint})/I_F(\text{tail}). \quad (1)$$

Descriptive statistics tests were used to compare different groups.

Differences between any two groups were tested for significance using the nonparametric Mann-Whitney U -test. Significance was assumed at $p < 0.05$.

Associations were tested by calculating Spearman correlation coefficients (r_s) (very high correlation: 0.9 to 1.0, high correlation: 0.7 to 0.89, moderate correlation: 0.5 to 0.69, low correlation: 0.3 to 0.49, and little or no correlation: 0.00 to 0.29). Significance was assumed at $p < 0.05$.

As graphic representation of the data, box plots were drawn, displaying the first and third quartiles and the median (second quartile). The ends of the whiskers mark the minimum and maximum of all data.

Statistical tests were performed using SPSS version 13.0 (SPSS Inc., Chicago).

3 Results

3.1 Arthritis Severity and NIRF Imaging before Therapy

The joints of the animals were assessed and graded according to the clinical severity of arthritis. Only four joints showed low-grade or moderate arthritis at this time (known model-related variability in the development of arthritis severity at disease

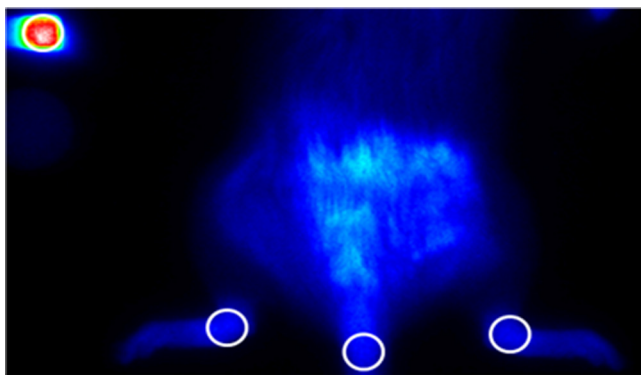


Fig. 1 Location of ROIs (white circles) for measurement of fluorescence intensities in ankle joints, tail, and reference cube.

onset)¹⁶ and were pooled for further statistical analysis (Fig. 2). The results revealed a statistically significant differentiation of control animals and animals with clinically apparent arthritis with respect to I_{NF} values (median I_{NF} : control 1.03, low to moderate 1.59, high 1.81) and a high correlation of the I_{NF} values with the clinical arthritis scores ($r_s = 0.860$). These data are in accordance with our previous findings in humans and experimental arthritis.^{11,14,21,22}

3.2 Group Allocation for Therapy

Due to the intrinsic variability in disease severity at onset, animals were assigned to the different groups based on the above-described arthritis grading at day 15:

Control: healthy rats without collagen injection and therapy (3 rats, $n = 6$ joints).

Meloxicam: CIA rats with clinically moderate to severe arthritic joints; these rats received 3 weeks of meloxicam treatment (4 rats, $n = 7$ joints).

No-therapy control: CIA rats with no or one arthritic joint; these rats only received symptomatic analgesic treatment with tramadol hydrochloride (4 rats, $n = 7$ joints).

Excluded: single joints of animals after collagen injection, which did not develop signs of arthritis within the period studied ($n = 8$ joints).

Six healthy joints from three animals without collagen injections comprised the control group (Table 1). Four CIA rats with clinical arthritis in seven joints were assigned to the meloxicam group. Another four CIA rats with clinical symptoms of arthritis in seven joints comprised the no-therapy control group. At the beginning of the treatment period, two animals of this group showed arthritis symptoms in two joints. During the study period, another five joints became symptomatic. Finally, a total of four animals with seven affected joints received analgesic treatment with tramadol hydrochloride. We excluded eight ankle joints from CIA rats that did not develop clinical

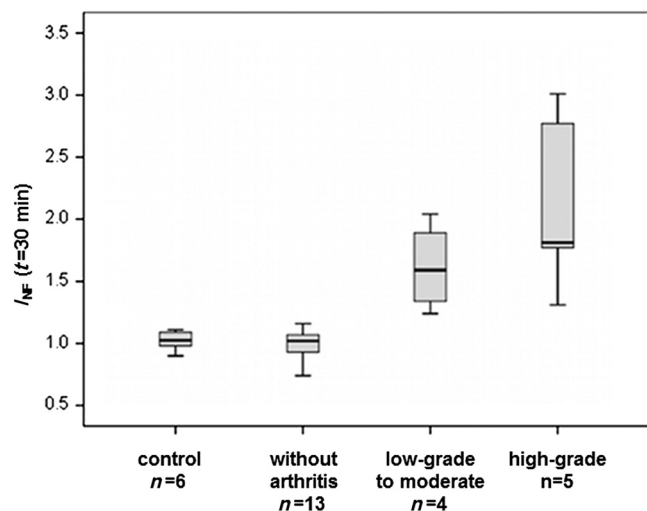


Fig. 2 Illustration of normalized fluorescence intensities (I_{NF}) of ankle joints 30 min after intravenous administration of TSC before therapy. Animals are grouped according to clinical arthritis scores.

Table 1 The numbers of joints with and without clinical arthritis in each group before and after therapy are shown. Eight ankle joints, from the meloxicam group ($n = 1$) and no-therapy control group ($n = 7$), which did not develop clinical arthritis throughout the treatment period, were excluded from further analysis (bold numbers in circles).

Group	Score	Control ($n = 6$)	Meloxicam ($n = 7$)	No-therapy control
Before therapy ($n = 28$)	With arthritis	–	7	2
	Without arthritis	6	①	12
After three weeks of therapy ($n = 28$)	With arthritis	–	6	7
	Without arthritis	6	2	⑦

arthritis during the study period from further analysis (bold numbers in circles, Table 1).

3.3 Arthritis Severity and NIRF Imaging after Therapy

Clinical scoring and *in vivo* NIRF imaging of all animals were repeated after 2 and 3 weeks of therapy. The I_{NF} values for the ankle joints were calculated from the fluorescence intensity data 30 min after TSC injection.

A statistically significant improvement of clinical arthritis symptoms from high- or moderate-grade to moderate- or low-grade scores became obvious in the meloxicam group ($n = 7$ joints) already after 2 weeks of treatment, while all ankle joints ($n = 7$) in the no-therapy control group (tramadol hydrochloride) showed statistically significant disease progression to high-grade scores with severe erythema and tissue swelling, which persisted throughout the study period (Table 2). The therapeutic success of meloxicam treatment, reflected by decreasing clinical scores, translated into decreasing I_{NF} values in NIRF imaging (median I_{NF} : pre-1.81, after 2 weeks of therapy 1.32, after 3 weeks of therapy 1.23). Moreover, disease progression, seen in the no-therapy control group, accordingly translated into increasing I_{NF} values (median I_{NF} : pre-1.04, after 2 weeks of therapy 1.63, after 3 weeks of therapy 1.66) (Fig. 3). Even more important, the correlation between I_{NF} values and

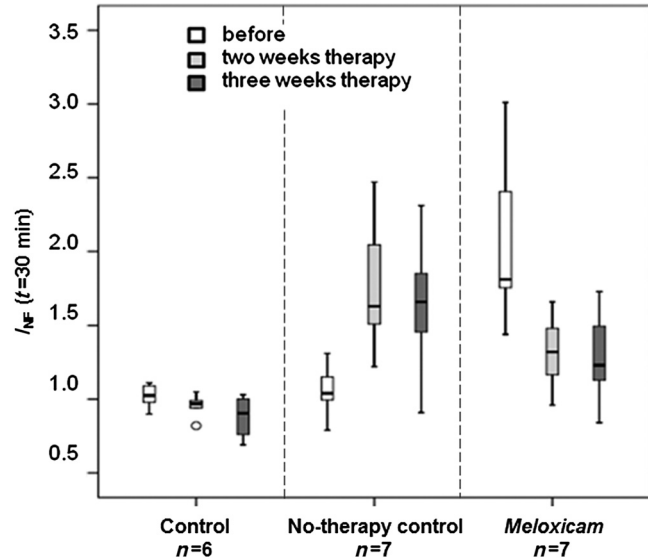


Fig. 3 Illustration of normalized fluorescence intensities (I_{NF}) of ankle joints by treatment group 30 min after intravenous TSC administration. The results after 2 and 3 weeks of therapy are shown in comparison to controls. The circle indicates an outlier. Eight ankle joints from the meloxicam group ($n = 1$) and no-therapy control group ($n = 7$), which did not develop clinical arthritis throughout the treatment period, were excluded from this analysis.

Table 2 Number of joints and their respective clinical arthritis score before and after 2 and 3 weeks of therapy. Eight ankle joints from the meloxicam group ($n = 1$) and no-therapy control group ($n = 7$), which did not develop clinical arthritis throughout the treatment period, were excluded from further analysis (bold numerals in circles).

Group	Score	Control ($n = 6$)	Meloxicam ($n = 7$)	No-therapy control ($n = 14$)
Before therapy	High-grade	0	4	1
	Low-grade to moderate	0	3	1
	Without arthritis	6	①	12
After two weeks of therapy	High-grade	0	0	7
	Low-grade to moderate	0	6	0
	Without arthritis	6	2	7
After three weeks of therapy	High-grade	0	0	7
	Low-grade to moderate	0	6	0
	Without arthritis	6	2	⑦

clinical scores was high or moderate, respectively, for each time point (before therapy: $r_s = 0.860$, after 2 weeks of therapy: $r_s = 0.825$, after 3 weeks of therapy: $r_s = 0.634$) as well as throughout the whole study ($r_s = 0.758$).

3.4 Treatment Effect

The clinical manifestation of arthritis and the histologically detectable destruction of the joints were statistically significantly reduced by the anti-inflammatory meloxicam therapy within 3 weeks. This therapeutic success could reliably be visualized by NIRF imaging using TSC.

3.5 Histology

After 3 weeks of treatment, all ankle joints were removed and investigated by histology to assess the presence and extent of arthritis symptoms such as synovial membrane hyperplasia, sub-synovial fibrosis of the surrounding loose connective tissue, inflammatory cell infiltration, and pannus formation (organized inflammatory exudate within the joint space).

Already at low magnification, the different grades of destruction in the ankle joints between treated animals and controls

became visible (Fig. 4). The ankle joints of control animals showed unchanged healthy joint structures. In contrast, the inflamed joints of animals after 3 weeks of meloxicam treatment revealed histological signs of moderate arthritis with synovial proliferation, synovial fibrosis, inflammatory cell infiltration, and pannus formation. All signs of chronic inflammatory arthritis were highly pronounced in animals with pain treatment only (Fig. 4).

4 Discussion

Our results confirm that fluorescence-enhanced NIRF imaging using the experimental cyanine dye TSC is a powerful approach to visualization of inflammation in arthritic joints *in vivo*. To our knowledge, the NIRF imaging study presented here for the first time successfully visualized the therapeutic effect of an anti-rheumatic drug in CIA rats over 3 weeks of treatment.

The investigated dye, TSC, has already shown its diagnostic potential for arthritis evaluation in an earlier study conducted by our group.¹⁴ Compared to the clinically used near-infrared (NIR) dye indocyanine green (ICG), TSC has superior characteristics with respect to an increased blood half-life (caused by higher hydrophilicity and lower protein binding) and a higher

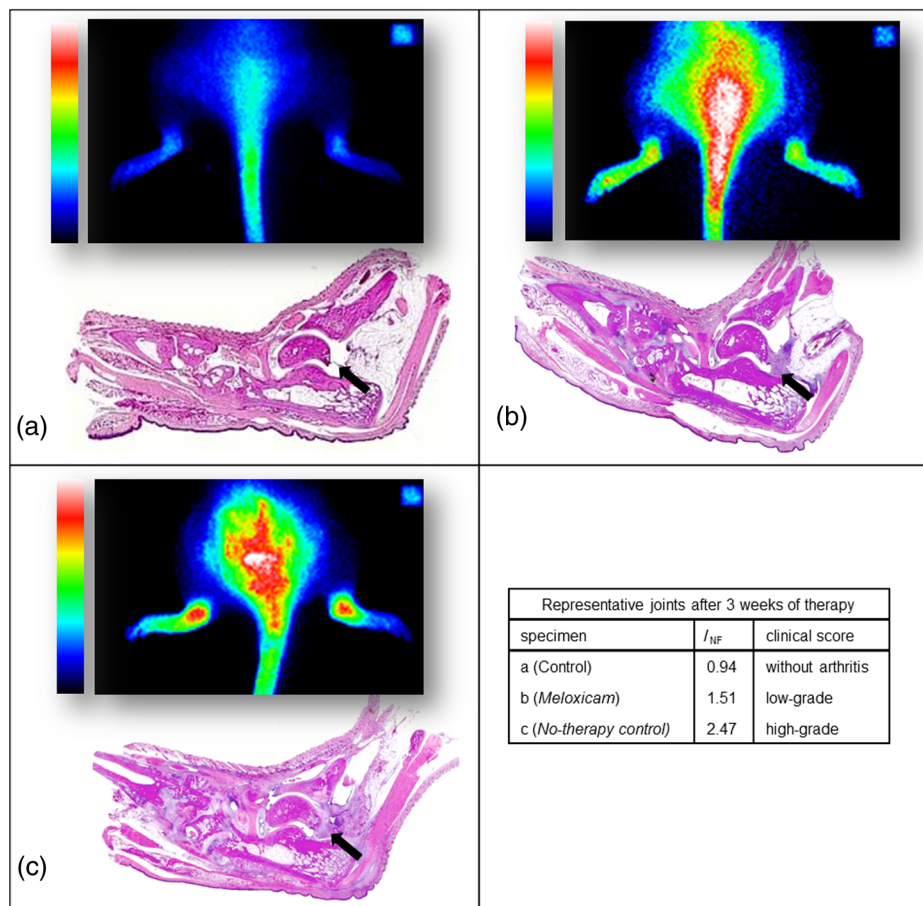


Fig. 4 Representative histological sections of ankle joints with corresponding NIRF images and I_{NF} values. Fluorescence images are shown in false colors (range 0 to 100,000 for all color bars) (a) Control animal without arthritis showing faint fluorescence in both ankle joints and normal histological structures (left joint); (b) animal after 3 weeks of meloxicam therapy with prominent fluorescence in both ankle joints revealing histological medium grade destruction of the joints (right joint); (c) ankle joints with persisting high-grade arthritis during analgesic tramadol hydrochloride treatment only, revealing severe histological joint destruction (right joint) and bright fluorescence. Fluorescence at the tail base is due to local inflammation at the site of intradermal collagen injection. The reference cube is visible in the right upper corner.

fluorescence quantum yield (10%) in aqueous media.^{19,20} This quantum yield leads to an eight times higher sensitivity in monitoring inflammation compared to ICG.¹⁴

Preferred rodent models for the joint pathology that occurs in human RA are adjuvant-induced (AIA), collagen-induced (CIA), and streptococcal-cell-wall-induced arthritis.¹⁶ These models have proven to predict the responsiveness of human RA patients. Structural and immunological changes in CIA best resemble RA, while AIA lesions are most severe and consistent.¹⁶ We chose the CIA model, as its joint changes not only resemble RA in humans but are also induced by the same factors that cause human RA.^{23–26} The incidence of CIA in Lewis rats varies from 60% to 90% across laboratories, and arthritis develops over approximately a 5-day period, usually starting 11 days after immunization.¹⁶ The variable and not fully predictable onset of arthritis in the CIA model has led to unequal numbers of joints in the different treatment groups and to the exclusion of joints in this study.⁸ However, this variety in arthritis severity at the onset of disease allowed us to select rats with definite arthritis for therapy monitoring in the meloxicam group, while pre-symptomatic or mildly to moderately affected animals were well suited to monitor disease progression in the no-therapy control group.

For the assessment of the severity of the arthritis, we used a 4-point grading scale with respect to consistency and comparability to our previous work and in agreement with our published papers.^{14,22} Moreover, this 4-point scale well matches the histological assessment of human synovitis score provided by Krenn et al.¹⁸ For the first time within the therapeutic period, we monitored the animals after 2 weeks, as from our experience, disease progression or amelioration typically become obvious after this time.

We have recently shown¹⁴ and herein reproduced the finding that TSC-induced I_{NF} signals are highly correlated ($r_s = 0.758$) with the arthritis grade throughout disease progression. Synovitis, a hallmark of arthritis, develops early in the disease process and can be visualized by NIRF-enhanced imaging using TSC. This approach is therefore suitable for diagnostic purposes and grading of disease activity. It has been assumed that the therapeutic efficacy of disease-modifying RA drugs will have an impact on inflammation as an early sign. Therefore, TSC-enhanced NIRF imaging was expected to have potential for therapy monitoring.

In fact, meloxicam treatment significantly improved ankle joint pathology, as confirmed by clinical scores in our study, and this therapeutic effect reliably translated into a decrease in fluorescence intensity values using TSC-enhanced NIRF imaging. In contrast, all arthritic joints of the no-therapy control group deteriorated to high-grade arthritis with high fluorescence intensities in NIRF imaging. For all rats and groups, the clinical scores and I_{NF} values revealed high correlation after 2 weeks of therapy, $r_s = 0.825$, and a moderate correlation after 3 weeks of therapy, $r_s = 0.634$. The correlation values decreased with disease progression. As described earlier, this animal model comprises both the acute (<2 weeks) and the chronic phases (>2 weeks) of arthritis.¹⁵ Although the acute phase is mainly characterized by inflammation, in chronic arthritis, bone, and cartilage remodeling as well as fibrotic processes come to the fore. Although inflammation plateaus in this phase, NIRF imaging still provides sufficient correlation for therapy monitoring.

A limitation of our study is that different numbers and small numbers of animals were available in the individual study

groups. As the dropout rate in the CIA model can be as high as 40%, animals can be assigned to the different study groups only after the first symptoms have appeared. In this study, only a few joints were assessed as mildly or moderately arthritic and were merged as “mild to moderate” for reasons of statistical analysis. For further studies, it would be desirable to have an equal distribution of animals with all different disease states in the respective groups. However, this will require a significant higher number of animals.

Recently, a study was published that used an AIA rat model for visualizing arthritis activity by NIRF imaging. Glucocorticoids were administered prior to disease onset, thereby successfully demonstrating their preventive potential. However, therapy monitoring in its literal sense was not addressed by this study.²⁷

5 Conclusion

Our results indicate that TSC-enhanced NIRF imaging of ankle joints is a powerful tool not only for diagnosis but also for therapy monitoring of arthritis in CIA rats. As the CIA rat model has already proven to be a model of high-translational value, the approach presented here has significant potential for preclinical development of future RA therapeutics.

For RA diagnosis in patients an NIRF imaging system and the approved dye ICG¹¹ (Xiralite®) are already commercially available. Compared to ICG, TSC has an eight times higher detection sensitivity¹⁴ and has already been used in the clinic for breast cancer imaging. NIRF imaging using TSC is assumed to be a promising modality for therapy monitoring in RA patients.^{28,29}

Acknowledgments

We acknowledge the excellent technical contribution of Robert Ivkic and Astrid Knop. The authors thank Bettina Herwig for language editing. This research was supported in part by the European Regional Development Fund (ERDF) and by the Investitionsbank Berlin (IBB).

References

1. D. L. Scott et al., “Rheumatoid arthritis,” *Lancet* **376**(9746), 1094–1108 (2010).
2. S. Merkesdal et al., “Indirect medical costs in early rheumatoid arthritis: composition of and changes in indirect costs within the first three years of disease,” *Arthritis Rheum.* **44**(3), 528–534 (2001).
3. F. Wolfe and D. J. Hawley, “The longterm outcomes of rheumatoid arthritis: work disability: a prospective 18 year study of 823 patients,” *J. Rheumatol.* **25**(11), 2108–2117 (1998).
4. D. Chamberland et al., “Optical imaging: new tools for arthritis,” *Integr. Biol.* **2**(10), 496–509 (2010).
5. L. E. Glynn, “Pathology, pathogenesis, and aetiology of rheumatoid arthritis,” *Ann. Rheum. Dis.* **31**(5), 412–420 (1972).
6. S. Gay et al., “Molecular and cellular mechanisms of joint destruction in rheumatoid arthritis: two cellular mechanisms explain joint destruction?,” *Ann. Rheum. Dis.* **52**(Suppl. 1), S39–S47 (1993).
7. J. M. Bathon et al., “A comparison of etanercept and methotrexate in patients with early rheumatoid arthritis,” *N. Engl. J. Med.* **343**(22), 1586–1593 (2000).
8. K. Ikeda et al., “Aspects of early arthritis. Biological therapy in early arthritis—overtreatment or the way to go?,” *Arthritis Res. Ther.* **9**(3), 211 (2007).
9. A. Rubbert-Roth and A. Finckh, “Treatment options in patients with rheumatoid arthritis failing initial TNF inhibitor therapy: a critical review,” *Arthritis Res. Ther.* **11**(Suppl. 1) (2009).

10. S. Vollmer et al., "Extra domain B fibronectin as a target for near-infrared fluorescence imaging of rheumatoid arthritis affected joints *in vivo*," *Mol. Imaging* **8**(6), 330–340 (2009).
11. T. Fischer et al., "Detection of rheumatoid arthritis using non-specific contrast enhanced fluorescence imaging," *Acad. Radiol.* **17**(3), 375–381 (2010).
12. R. Meier et al., "Synovitis in patients with early inflammatory arthritis monitored with quantitative analysis of dynamic contrast-enhanced optical imaging and MR imaging," *Radiology* **270**(1), 176–185 (2014).
13. S. G. Werner et al., "Inflammation assessment in patients with arthritis using a novel *in vivo* fluorescence optical imaging technology," *Ann. Rheum. Dis.* **71**(4), 504–510 (2012).
14. I. Gemeinhardt et al., "Near-infrared fluorescence imaging of experimentally collagen-induced arthritis in rats using the nonspecific dye tetrasulfocyanine in comparison with gadolinium-based contrast-enhanced magnetic resonance imaging, histology, and clinical score," *J. Biomed. Opt.* **17**(10), 106008 (2012).
15. M. Stolina et al., "The evolving systemic and local biomarker milieu at different stages of disease progression in rat collagen-induced arthritis," *Biomarkers* **13**(7), 692–712 (2008).
16. B. Bolon et al., "Rodent preclinical models for developing novel anti-arthritis molecules: comparative biology and preferred methods for evaluating efficacy," *J. Biomed. Biotechnol.* **2011**, 569068 (2011).
17. U. Busch and G. Engelhardt, "Distribution of [¹⁴C]meloxicam in joints of rats with adjuvant arthritis," *Drugs Exp. Clin. Res.* **16**(2), 49–52 (1990).
18. V. Krenn et al., "Grading of chronic synovitis—a histopathological grading system for molecular and diagnostic pathology," *Pathol. Res. Pract.* **198**(5), 317–325 (2002).
19. K. Licha et al., "Hydrophilic cyanine dyes as contrast agents for near-infrared tumor imaging: synthesis, photophysical properties and spectroscopic *in vivo* characterization," *Photochem. Photobiol.* **72**(3), 392–398 (2000).
20. C. Perlitz et al., "Comparison of two tricarbo-cyanine-based dyes for fluorescence optical imaging," *J. Fluoresc.* **15**(3), 443–454 (2005).
21. T. Dziekan et al., "Detection of rheumatoid arthritis by evaluation of normalized variances of fluorescence time correlation functions," *J. Biomed. Opt.* **16**(7), 076015 (2011).
22. T. Fischer et al., "Assessment of unspecific near-infrared dyes in laser-induced fluorescence imaging of experimental arthritis," *Acad. Radiol.* **13**(1), 4–13 (2006).
23. F. H. Durie et al., "Collagen-induced arthritis as a model of rheumatoid arthritis," *Clin. Immunol. Immunopathol.* **73**(1), 11–18 (1994).
24. J. M. Stuart et al., "Type II collagen-induced arthritis in rats. Passive transfer with serum and evidence that IgG anticollagen antibodies can cause arthritis," *J. Exp. Med.* **155**(1), 1–16 (1982).
25. D. E. Trentham "Collagen arthritis as a relevant model for rheumatoid arthritis," *Arthritis Rheum.* **25**(8), 911–916 (1982).
26. D. E. Trentham et al., "Autoimmunity to type II collagen an experimental model of arthritis," *J. Exp. Med.* **146**(3), 857–868 (1977).
27. F. Dietzel et al. "Assessment of rat antigen-induced arthritis and its suppression during glucocorticoid therapy by use of hemicyanine dye probes with different molecular weight in near-infrared fluorescence optical imaging," *Invest. Radiol.* **48**(10), 729–737 (2013).
28. A. Poellinger et al., "Breast cancer: early- and late-fluorescence near-infrared imaging with indocyanine green—a preliminary study," *Radiology* **258**(2), 409–416 (2011).
29. A. Poellinger et al., "Near-infrared imaging of the breast using omocianine as a fluorescent dye: results of a placebo-controlled, clinical, multi-center trial," *Invest. Radiol.* **46**(11), 697–704 (2011).

Sonja Vollmer received her PhD in biochemistry from Free University Berlin, Germany. She started her scientific career with Schering AG, later Bayer AG. Her activities covered the field of diagnostic imaging in a variety of modalities, MRI, CT, PET, NIRF. She is now working as a laboratory head in Common Mechanism Research.

Ines Gemeinhardt is a postdoctoral researcher at the Charité—Universitätsmedizin Berlin in Germany. She received her PhD at the Institute of Veterinary Anatomy, Faculty of Veterinary Medicine, Freie Universität Berlin Veterinary Medicine in March 2005. Her current main research interests are on iron oxide nanoparticle for MR imaging, magnetic particle imaging, and near-infrared imaging.

Axel Vater received his training as an engineer in biotechnology at the Technische Universität Berlin, Germany, with a research semester at Harvard Medical School. During his doctoral thesis, he specialized in therapeutic nucleic acid aptamers. Although working as a research scientist at Bayer Schering Pharma, he focused on discovery of targeted and smart optical imaging probes. Subsequently, he returned to therapeutics, now serving as vice president for drug discovery at NOXXON Pharma AG in Berlin, Germany.

Beatrix Schnorr is a postdoctoral researcher at the Charité—Universitätsmedizin Berlin, Germany. She received her PhD in veterinary medicine at the Freie Universität of Berlin in 1999. Her current main research interests are on iron oxide nanoparticles, MR imaging, magnetic particle imaging and near-infrared imaging. She also has interest in investigation of drug-coated balloons which inhibit restenosis due to neointimal proliferation in coronary and peripheral arteries.

Jörg Schnorr is a postdoctoral researcher at the Charité—Universitätsmedizin Berlin, Germany. He received his PhD in veterinary medicine at the Free University of Berlin in 1998. His current main research interests are on iron oxide nanoparticles, MR imaging, magnetic particle imaging, computer tomography, ultrasound imaging and near-infrared imaging. He also has interest in investigation of relationship between imaging agents and glycosaminoglycans.

Jan Voigt received his degree as engineer in physical engineering in 2003 at University of Applied Sciences in Brandenburg. In addition, he received a Master of Science in medical physics at Technical University of Kaiserslautern in 2010. Currently, he is working in the Department of Radiation Therapy and Special Oncology at Medical University of Hannover.

Bernd Ebert was a senior scientist at the Department of Biomedical Optics, PTB Berlin, Germany. He received his PhD in biophysics from the Academy of Sciences Berlin, Germany. His activities covered the field of time-resolved fluorescence imaging and the development of spectroscopic devices as well as algorithms for image evaluation and data processing. In the last years, he developed a novel optical method for early detection of rheumatoid arthritis.